arXiv:cond-mat/0105250v1 [cond-mat.str-el] 13 May 2001

Geometric frustration and magnetization plateaus in quantum spin and Bose-Hubbard models on tubes

Dmitry Green[a] and Claudio Chamon[b]
[a] *Department of Physics, Yale University, New Haven, CT 06520*
[b] *Department of Physics, Boston University, Boston, MA 02215*

We study XXZ Heisenberg models on frustrated triangular lattices wrapped around a cylinder. In addition to having interesting magnetic phases, these models are equivalent to Bose-Hubbard models that describe the physical problem of adsorption of noble gases on the surface of carbon nanotubes. We find analytical results for the possible magnetization plateau values as a function of the wrapping vectors of the cylinder, which in general introduce extra geometric frustration besides the one due to the underlying triangular lattice. We show that for particular wrapping vectors $(N,0)$, which correspond to the zig-zag nanotubes, there is a macroscopically degenerate ground state in the classical Ising limit. The Hilbert space for the degenerate states can be enumerated by a mapping first into a path in a square lattice wrapped around a cylinder (a Bratteli diagram), and then to free fermions interacting with a single $\mathbf{Z}_N$ degree of freedom. From this model we obtain the spectrum in the anisotropic Heisenberg limit, showing that it is gapless. The continuum limit is a $c=1$ conformal field theory with compactification radius $R=N$ set by the physical tube radius. This result cannot be checked against a Lieb-Schultz-Mattis argument, for the argument is inconclusive when applied to this problem. We show that the compactification radius quantization is exact in the projective $J_\perp/J_z \ll 1$ limit, and that higher order corrections reduce the value of R. The particular case of a $(N=2,0)$ tube, which corresponds to a 2-leg ladder with cross links, is studied separately and shown to be gapped because the fermion mapped problem contains superconducting pairing terms.

PACS: 67.70+n, 71.10.Pm, 75.10.Jm

I. INTRODUCTION

There has been growing interest in one-dimensional quantum spin chains and ladders that display magnetization plateaus when subjected to an external magnetic field [1–7]. This requires materials with exchange couplings within a range for which the necessary external fields are attainable in the laboratory. Examples are the spin $S=1$ nickel compound [Ni(Medpt)$_2$(μ-ox)(μ–N$_3$)]ClO$_4$·0.5H$_2$O, which displays a plateau at $\langle M\rangle = 1/2$ [8], and the spin $S=1/2$ compound NH$_4$CuCl$_3$, which displays plateaus with magnetization $\langle M\rangle = 1/4, 3/4$ [9] (the magnetization is measured as a fraction of the maximum magnetization *per* spin S). One of the most interesting features in these systems is the possibility of gapless plateaus even in integer spin systems [3].

An important ingredient to obtain the plateaus is a p-merization, or the presence of periodic structures that allow for ground states with non-zero $\langle M\rangle$ other than the trivial cases $\langle M\rangle = \pm 1$. A particular case of a p-merized structure is a "spin tube", like the one proposed theoretically by Cabra, Honecker, and Pujol [5], and by Citro, Orignac, Andrei, and co-workers [6,7]. These tubes basically consist of p-leg spin ladders with periodic boundary conditions coupling the 1st and pth chains. Although interesting structures from a theoretical perspective, these tubes are not yet realizable experimentally.

In this paper we explore another type of spin tube, which is formed by wrapping a triangular lattice on a cylinder. The triangular lattice with anti-ferromagnetic couplings is frustrated, and, depending on the wrapping vector, extra geometric frustrations are introduced. One motivation to study such types of spin tube lattices is that they are realized physically in monolayer adsorption of noble gases on the surface of carbon nanotubes. This paper contains a detailed account of the results in Ref. [10], as well as new analytical results that explain the numerical findings of the previous work.

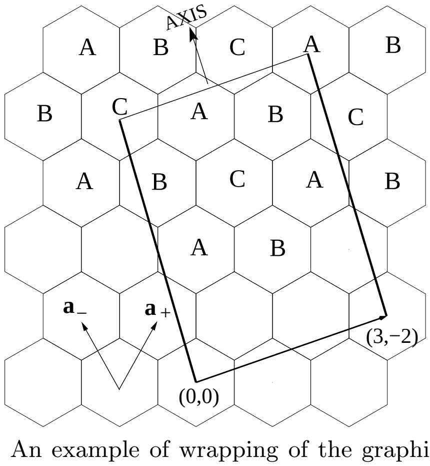

FIG. 1. An example of wrapping of the graphite sheet to make a $(3,-2)$ tube. $\vec{a}_\pm$ are the primitive lattice vectors of the honeycomb lattice. The solid rectangle is the supercell of the tube. Also shown is the tripartite labeling A, B, C.

The lattice sites for the spin tubes we consider can be described by a pair of integers (N, M), exactly the notation for carbon nanotubes, for which the following nomenclature applies: (N, N) are called armchairs, $(N, 0)$ are zig-zags, and the general case are chiral. The triangular lattice points are the centers of the hexagonal lattice of the nanotubes (the adsorption centers), as shown in Fig. 1. The integers (N, M) define the wrapping vector of the honeycomb lattice that identifies the origin with the point $N\vec{a}_+ + M\vec{a}_- \equiv 0$, where $\vec{a}_\pm$ are the primitive lattice vectors of the honeycomb lattice.

The tripartite nature of the triangular lattice of adsorption sites is destroyed whenever the wrapping vector (N, M) is such that $N - M$ is not divisible by 3. An example of a $(7, 0)$ tube is presented in Ref. [10], and reproduced below in Fig. 2.

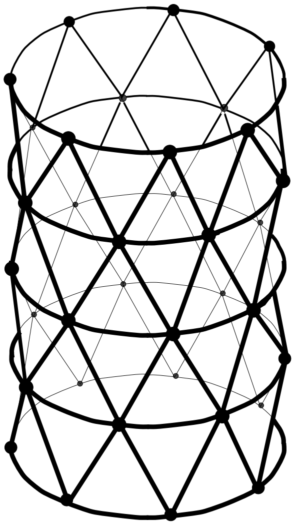

FIG. 2. Adsorption sites on a $(7, 0)$ zig-zag nanotube

The problem of adsorption of noble gases onto planar graphite can be understood within a lattice gas model, with the hexagonal substrate providing adsorption sites that form a triangular lattice [11]. This problem is equivalent to a Bose-Hubbard model, where a large nearest neighbor repulsion arises from the fact that even the smaller of noble gas atoms, helium, spread over an area larger than that of the carbon hexagons (the characteristic length scale for the zero-point motion of the He atom comes from the Lennard-Jones potential length scale σ=2.56Å, while the separation between C atoms in the hexagons is 1.42Å) [12]. The potential energy for atoms to be adsorbed in the same site are even larger, and thus we take the hard-core boson limit. The case of adsorption on the nanotube geometry is similar once the periodicity condition due to the wrapping vector (N, M) is considered.

The lattice gas is defined by the Bose-Hubbard Hamiltonian [13,14]

$$\mathcal{H} = -t \sum_{\langle ij \rangle} (b_i^\dagger b_j + b_j^\dagger b_i) + V \sum_{\langle ij \rangle} n_i n_j - \mu \sum_i n_i \ , \quad (1)$$

where n_i is the boson density at site i, V is the nearest neighbor repulsion and t is the hopping amplitude. In the equivalent Heisenberg spin representation,

$$\mathcal{H} = -J_\perp \sum_{\langle ij \rangle} \left(S_i^x S_j^x + S_i^y S_j^y \right) - J_z \sum_{\langle ij \rangle} S_i^z S_j^z - H \sum_i S_i^z \quad (2)$$

where $S_i^z = n_i - 1/2$, $J_\perp = 2t$, $J_z = -V$, and $H = \mu - 3V$ is an effective external magnetic field. The equivalence between the hard core Bose-Hubbard model and the XXZ Heisenberg spin $S = 1/2$ model allows us to study both physical problems of the magnetization properties of the spin tube and the adsorption of noble gases on carbon nanotubes at the same time.

In the adsorption problem one finds filling fraction plateaus as a function of the chemical potential; this is the counterpart of the magnetization plateau in the spin models as a function of external magnetic field. The filling fraction plateaus most often correspond to solid phases, with an energy gap in the excitation spectrum. However, as we show in this paper, there are examples of gapless plateaus which occur in the case of $(N, 0)$ tubes (zig-zags) with N not divisible by 3. These plateaus correspond to a compressible correlated fluid, which is described by a $c = 1$ conformal field theory with compactification radius $R = N$.

Many of the interesting results we find in the study of the spin tubes come from the geometric frustration that is introduced when the lattice is wrapped up into a cylinder. In some cases, one can think of the boundary conditions as forcing a single domain wall running along the tube. Recently, Henley and Zhang [15] have studied the nearest neighbor Hubbard model for spinless fermions as a toy model for understandying stripe phases when the system is doped away from half-filling. The situation is very similar to our case.

The paper is organized as follows. In section II we study the classical limit when the hopping t in the Bose-Hubbard model goes to zero; in spin language, this corresponds to the Ising limit. We explain a macroscopic degeneracy present in the frustrated $(N, 0)$ zig-zag tubes. In section III we turn on the quantum hopping term t (or the XY spin couplings $J_\perp = 2t$). We sumarize our findings in section IV, where we also discuss possible experimental signatures of the plateaus.

II. CLASSICAL LIMIT

We start our analysis in the simpler classical limit, which corresponds to the Ising limit $J_\perp = 0$. In the Bose-Hubbard model it is the no-hopping limit $t = 0$.

We will carry out the discussion interchangeably between the Bose-Hubbard and spin languages.

Without loss of generality, we take the integers $N, M > 0$; all other cases can always be brought to this form by a rotation of the basis vectors $\vec{a}_\pm$ by multiples of 60°. The triangular lattice sites can be partitioned into three interpenetrating sublattices that we label by A, B, and C. If we define $q \equiv (N-M)(\text{mod } 3)$, then the wrapping of the lattice does not break this tripartite property if $q = 0$.

Let us begin by studying the commensurate case ($q = 0$) before we continue to the more interesting incommensurate cases ($q = 1, 2$). As a function of the chemical potential, the possible filling fractions are $\nu = 0, 1/3, 2/3$, and 1, corresponding to the cases of no filling, one sublattice filled, two sublattices filled, or all three sublattices filled. Notice that there is a threefold ground state degeneracy for $\nu = 1/3$ from filling any one of the three sublattices; similarly, there is a threefold degeneracy for $\nu = 2/3$ from filling all but one of the three sublattices. The only values of chemical potential for which there is a macroscopic degeneracy in the $q = 0$ case is right at the transition points between plateaus. In the spin language, the filling fractions correspond to magnetizations $\langle M\rangle = -1, -1/3, 1/3$, and 1. A schematic plot of the magnetization as a function of the external field H is shown in Fig. 3

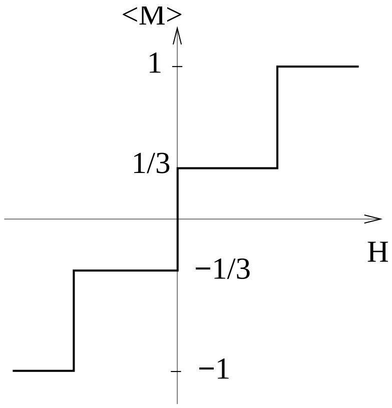

FIG. 3. Schematic representation of the magnetization (or filling) plateaus for a $q = 0$ commensurate tube ($T = 0$).

Let us now analyze the incommensurate cases $q = 1, 2$. One still obtains the trivial plateaus at $\nu = 0, 1$, but the question is what happens to the partially filled plateaus. Here we describe an analytical argument that leads to the possible filling fractions for general (N, M). In this derivation, we make some assumptions based on physical intuition, which is supported by exact numerical transfer matrix calculations for a range of values for N, M. First, one can separate the lattice sites into three classes locally, but not globally; there will always be a topological line defect running along the tube for $q = 1, 2$. We call this line the "zipper"; examples are shown in Fig. 4 for a $(4, 0)$ tube. One can open up the tube along the zipper, and label the hexagons centered at the triangular lattice points A, B,and C. However, now the number of A, B, and C points are no longer all equal. Filling only one of these three classes of points leads to filling fractions ν that depend on the zipper geometry, and on which of A, B, or C were chosen. For example, a case leading to filling fractions $\nu = 7/20, 3/10$ is shown in Fig. 4a, and another leading to filling fractions $\nu = 1/2, 1/4$ is shown in Fig. 4b.

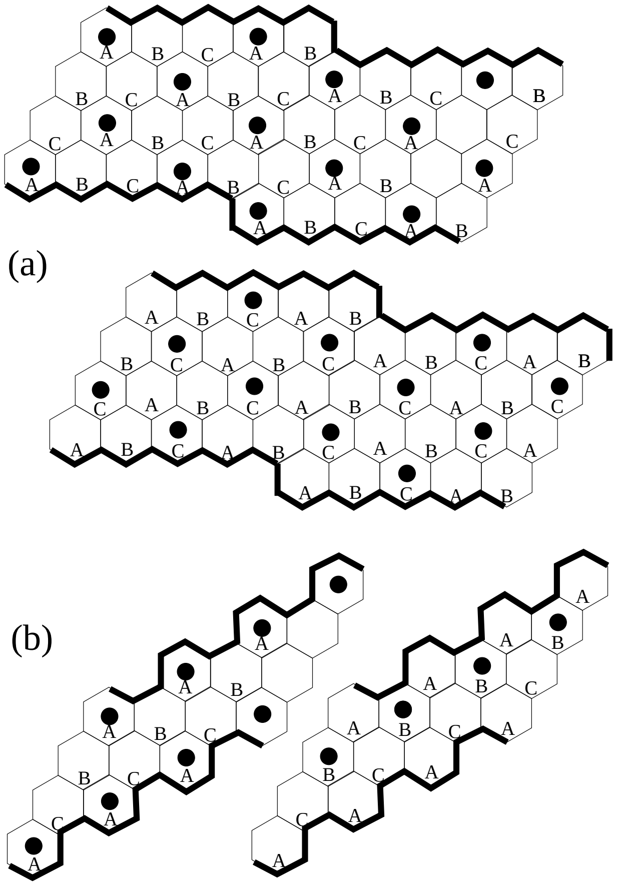

FIG. 4. Two examples of zippers for a $(4, 0)$ tube. When the tube is opened up along the zipper (thick lines), the hexagonal lattice can be separated locally into three sublattices A, B, and C. By filling the sublattices labelled by A, B, and C one obtains for case (a) either $\nu = 7/20$ if A or B is chosen, or $\nu = 3/10$ if C is chosen. For case (b), one obtains $\nu = 1/2$ if A is chosen, or $\nu = 1/4$ if B or C is chosen.

There is an infinite number of possible zippers for a given (N, M). In order to choose the one that leads to the lowest energy state, we argue that the zipper must be as straight as possible. The rationale is that bending the zipper should cost energy. So zippers as in Fig. 4b should be preferred. For a given wrapping vector (N, M), $N, M > 0$, we then investigate two zippers that we label by two vectors $\vec{z}_1 = (1, -2)$ and $\vec{z}_2 = (2, -1)$. These two vectors differ by a rotation of 60°, and are shown in Fig 5. A third $\vec{z}_3 = (1,1)$ is not considered because for $N, M > 0$ this zipper winds rapidly around the tube, and hence there is a large energy cost associated with its longer length.

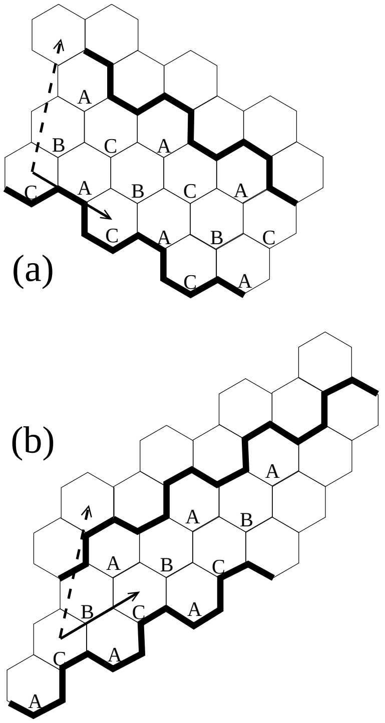

FIG. 5. Two straight zippers in the (2, 1) chiral tube, labeled by the vectors (solid arrows) $\vec{z}_1 = (1,-2)$ in (a) and $\vec{z}_2 = (2,-1)$ in (b). The wrapping vectors is the dotted arrow.

To proceed, we must calculate the boundary energy cost associated with the topological mismatch on the two sides of the zipper. Consider the portion of a tube shown in Fig 6, for a $(2,-1)$ zipper, where in each hexagon we write its coordinates (i, j) in the $\vec{a}_\pm$ basis.

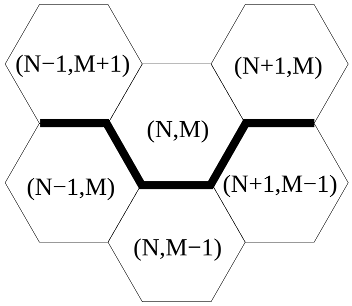

FIG. 6. Labelling of the hexagons by their coordinates in the $\vec{a}_\pm$ basis for the $(2,-1)$ zipper. The zipper is shown as a dark line. The region below the line lies within the boundaries of the unwrapped tube.

Within the boundaries set by the zipper, we can label the sites A, B, and C according to:

$$i - j \equiv \begin{cases} 0 \pmod 3 \to A \\ 1 \pmod 3 \to B \\ 2 \pmod 3 \to C \end{cases} . \tag{3}$$

In Fig. 7 we show the possible boundary configurations for $q = 0, 1, 2$. Let n_b be the number of near neighbors that are now both occupied *per* unit length, $|\vec{z}_2|$, along the zipper. (We also refer to the situation of occupied near neighbor sites as a *bond* between the sites). For $q = 0$, $n_b = 0$ since the tripartite lattice is not frustrated, but

- for $q = 1$, $n_b = 0$ if B or C is the filled (minority) sublattice; $n_b = 2$ if A is the filled (majority) sublattice.
- for $q = 2$, $n_b = 0$ if C is the filled (minority) sublattice; $n_b = 1$ if A or B is the filled (majority) sublattice.

Each set of occupied neighbors costs energy V. The energy $E(\nu)$ *per* area $\mathcal{A}$ for a given filling configuration is

$$\frac{E(\nu)}{\mathcal{A}} = \frac{n_b V}{\mathcal{A}} - \nu\mu \,, \tag{4}$$

where $\mathcal{A}$ is the supercell area given by

$$\begin{aligned} \mathcal{A} &= (N\vec{a}_+ + M\vec{a}_-) \cdot \vec{z}_2 \\ &= (N\vec{a}_+ + M\vec{a}_-) \cdot (2\vec{a}_+ - \vec{a}_-) \\ &= (2M + N)\mathcal{A}_{\text{hex}} \end{aligned} \tag{5}$$

and $\mathcal{A}_{\text{hex}} = |\vec{a}_\pm|^2\sqrt{3}/2$ is the area of one hexagon, which we will set to unity.

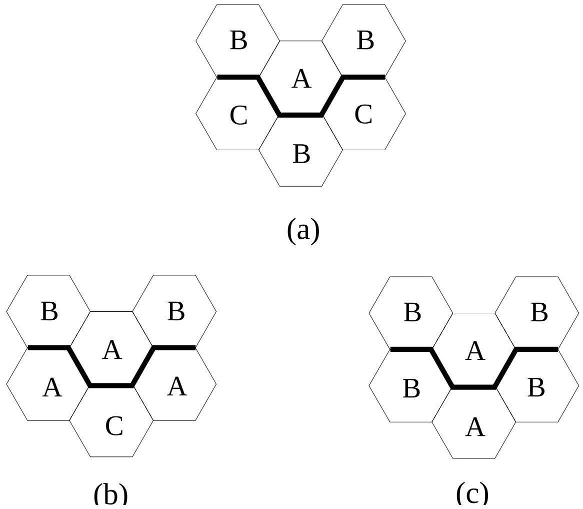

FIG. 7. The boundary configurations for the zipper $\vec{z}_1 = (2,-1)$ and the cases (a) $q = 0$, (b) $q = 1$, and (c) $q = 2$. The hexagons below the solid line lie within the boundaries set by the zipper and are labeled according to eqn. (3). Above the solid line, $(N, M) \equiv (0, 0)$ is labeled by A, while $(N-1, M+1), (N+1, M) \equiv (1, 0)$ are labeled by B.

Given that the number of A, B, and C lattice points are not all equal for $q \neq 0$, the possible filling fractions depend on the choice of filling either majority or minority lattice points. It is simple to check that

$$\nu_{+} = \frac{\lceil \mathcal{A}/3 \rceil}{\mathcal{A}} \quad \text{for majority filling} \tag{6}$$

$$\nu_{-} = \frac{\lfloor \mathcal{A}/3 \rfloor}{\mathcal{A}} \quad \text{for minority filling} \tag{7}$$

These fillings can be converted to magnetization values by $m_{\pm} = \langle M \rangle = 2\nu_{\mp} - 1$ and $H = \mu - 3V$. Notice that the spin flip symmetry $m \to -m$ corresponds to the particle-hole symmetry $\nu \to 1 - \nu$.

From this point on, the analysis is straightforward; one has to consider the energy density $E(\nu)/\mathcal{A}$ for *all* the different possibilities $q = 1, 2$, zippers $\vec{z}_{1,2}$, as well as majority or minority fillings $\nu_{\pm}$. The transition between ν_{+} and ν_{-} occurs at a critical field H_c when $E(\nu_{+}) = E(\nu_{-})$. After considering the eight cases, we obtain the minimum energy configurations for a generic (N, M) tube with $q = 1$:

$$m_{+} = \frac{1}{3}\left(1 + \frac{2}{2M + N}\right) \quad m_{-} = \frac{1}{3}\left(1 - \frac{2}{2N + M}\right)$$

$$H_c = \left(4 - \frac{2M}{N + M}\right) V \tag{8}$$

The complementary case of $q = 2$ is obtained by interchanging $N \leftrightarrow M$. We have verified the magnetizations and critical fields of eqn. (8) for small values of N, M previously [10].

Notice that we recover the graphite (planar) result $m_{\pm} = \pm 1/3$ as the tube radius approaches infinity $(N, M \to \infty)$, as we should.

A. Macroscopic Degeneracy

Most plateaus for general (N, M) tubes have only a discrete degeneracy corresponding to filling different sublattices. There is a macroscopic degeneracy only at the transition points. However, a careful consideration of the plateaus in the exceptional case of the frustrated zig-zag $(N, 0)$ tubes reveals that either the m_{+} or m_{-} plateau is macroscopically degenerate for its whole range of stability as a function of chemical potential (or magnetic field). Which plateau is degenerate depends on the the value of q.

Let us reconsider the ν_{+} filling of the $(5, 0)$ tube in Fig. 8. Imagine building a typical ν_{+} state layer-by-layer from top to bottom, with a total of L layers. Each new layer must add exactly two filled sites and one nearest-neighbor pair of occupied sites (1 bond). There are two ways to achieve this constraint. A non-trivial one is such that no two adjacent sites may be occupied within a layer, and this is the case shown in Fig. 8 (left). Notice that moving a particle from a layer to another adds another intra-layer bond. There is also a trivial one where two adjacent sites are occupied within a layer, and to conserve n_b, two adjacent sites must be occupied in the next, and so on down the tube. However, the class of such trivial states is only 5-fold degenerate, as opposed to the macroscopically degenerate class containing the state shown in Fig. 8. We now turn to the enumeration of the non-trivial class of states.

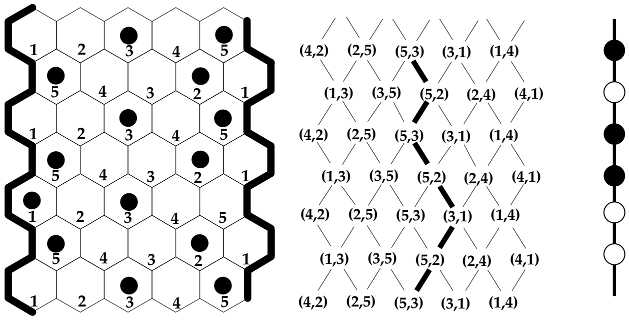

FIG. 8. LEFT: Typical configuration in ν_{+} (or m_{-}) of the $(5, 0)$ tube. Alternating numbering within layers allows a symmetric description from bottom-to-top or top-to-bottom. CENTER: Allowed states as paths on a wrapped square lattice. The vertex labels may be dropped. RIGHT: Steps to the right can be represented by particles (solid circles), and to the left by holes (open circles).

An allowed state can be represented as a string of occupied sites, $\sigma = \{\sigma_i\}$, $i = 1, \ldots, L$, which in our example is $\sigma = \{\cdots (5,3)(5,2)(5,3) \cdots\}$. At each layer, there are exactly two possibilities for the following one. For example, $(1,4)$ can be followed by $(1,4)$ or by $(2,4)$. However, the total number of possibilities at any given level is five. Fig. 8 (center) summarizes this structure succinctly as a *square* lattice wrapped on the cylinder. A typical state, then, is a lattice path along the tube. A path on this type of lattice is known as a Bratteli diagram. There is a recent Hubbard model considered by Henley and Zhang [15] of spinless fermions on a square lattice in which the bookkeeping of states is very similar.

Generalizing to $(N, 0)$, we find N possible states in each layer and two in the succeeding one, and the structure of states is again that of a wrapped Bratteli diagram with N sites along the circumference. The dimension of the Hilbert space is the number of lattice paths, $N 2^{L}$, so that in an infinitely long tube, the entropy per site (in the thermodynamic $L \to \infty$ limit) is exactly $S = (\ln 2)/N$. Notice that constrained paths introduce correlations along the length of the tube, despite the absence of inter-layer hopping.

The preceeding discussion is valid for all N with $q = 2$, where the macroscopically degenerate plateau occurs at

ν_+. For $q = 1$, the only modification is that the macroscopically degenerate plateau has filling ν_-.

III. QUANTUM LIMIT

Having understood in detail the classical limit, we now turn on a small hopping, $t \ll V$, that introduces quantum fluctuations. Away from the transitions, adding a particle necessarily increases n_b so that all plateaus begin with a classical gap of order V. Consequently, we can project to the Hilbert space of the classical ground states. Those plateaus which have only a discrete symmetry must retain their gaps, but the macroscopically degenerate plateaus are more complicated.

The matrix elements of the projected Hamiltonian (1) connect only those states that differ by a single hop of a boson:

$$\langle\sigma'|\mathcal{H}|\sigma\rangle = \begin{cases} -2t & \text{if} \quad \sum_i \delta_{\sigma_i\sigma_i'} = L-1 \\ 0 & \text{otherwise,} \end{cases} \tag{9}$$

where σ, σ' are two paths in the Bratteli lattice constructed in Section II A.

It turns out that this Hamiltonian is exactly solvable, being closely related to a class of solid-on-solid models that were introduced by Pasquier [17]. In the following, we derive the continuum limit of $\mathcal{H}$ directly.

In the previous section, the paths σ were labeled, for clarity, by a string of occupied sites on the nanotube. A simpler representation is to work with the wrapped square lattice directly, where the path is uniquely specified by an initial point and its direction in each layer. We will label the topmost layer by $i = 1$ with i increasing by 1 with each downward move. There are L layers of hexagons and we impose periodic boundary conditions, $L + 1 \equiv 1$. In order for the layers to match, L has to be even.

To specify the initial point on σ, we chose an "anchor" α on one of the N sites in the $i = 1$ layer ($\alpha = 1, \ldots, N$). Now, we represent a step to the right in layer i by a fermion, and a step to the left by a hole. We define fermion creation and anihilation operators $c_i^\dagger$ and c_i for each layer i. A state $|\sigma\rangle$ in the Hilbert space, S, is represented by

$$|\sigma\rangle = |\alpha\rangle \otimes c_{i_1}^\dagger c_{i_2}^\dagger \cdots c_{i_p}^\dagger |0\rangle \ , \tag{10}$$

where α is the anchor site in the first layer and $i_1 \cdots i_p$ are the layers where the path steps to the right. For instance, the portion of the path in Fig. 8 is $|\sigma\rangle = |3\rangle \otimes c_1^\dagger c_3^\dagger c_4^\dagger \cdots |0\rangle$. The fermionic representation is convenient since there is exactly one step in each layer, but hard-core bosons can also be used, as in one dimension they are equivalent. The number of particles (steps to the right) and holes (steps to the left) must add up to L (the total number of steps). Each path also has a topological character for the number of times that it winds around the tube, which must be a multiple of N in order for the path to close with the periodic boundary condition $L + 1 \equiv 1$. These two requirements are summarized by

$$N_p + N_h = L \tag{11}$$

$$N_p - N_h = bN \ , \tag{12}$$

where $N_{p,h}$ is the number of particles or holes, and b is the winding number (positive or negative). If each particle (hole) is assigned a positive (negative) unit charge, then bN is the total charge. Notice that $b = 0$ at half-filling ($N_p = N_h = L/2$).

Whenever it is allowed within a layer, a single hop changes the step sequence right-left to left-right and *vice versa*, which corresponds to $c_{i+1}^\dagger c_i$ or $c_i^\dagger c_{i+1}$. In a layer without a kink no hops are possible, and the hopping terms vanish by fermionic statistics. Since we are working in periodic boundary conditions, the boundary terms, $c_1^\dagger c_L$ and $c_L^\dagger c_1$, must be treated more carefully. A hop at this point is necessarily accompanied by a translation of the anchor point by $|\alpha\rangle \mapsto |\alpha \pm 1\rangle$. Let us represent this operation by

$$R_\pm|\alpha\rangle = |\alpha \pm 1\rangle \tag{13}$$

with $R_-^\dagger = R_+$. Cylindrical wrapping requires a $\mathbf{Z}_N$ symmetry because $|\alpha \pm N\rangle \equiv |\alpha\rangle$, *i.e.* $R_\pm^N = R_\pm$. Putting the bulk and boundary hopping terms together, the Hamiltonian of eqn. (9) becomes

$$\mathcal{H} = -2t \left[\sum_{i=1}^{L-1} c_{i+1}^\dagger c_i + R_- \otimes c_1^\dagger c_L \right] + h.c. \ . \tag{14}$$

We can think of $\mathcal{H}$ as describing free fermions on a periodic one dimensional chain with a $\mathbf{Z}_N$ impurity on one of the bonds.

$\mathcal{H}$ can be diagonalized exactly in momentum space. Going around the tube lengthwise contributes a phase e^{ikL} while going around the perimeter contributes $e^{i\phi}$, with $\phi = 2\pi a/N$ ($a = 1, \ldots, N-1$). Therefore toroidal boundary conditions require

$$e^{ikL} e^{i\phi} = 1 \ . \tag{15}$$

Or,

$$k = \frac{2\pi v}{L}\left(n + \frac{a}{N}\right) \ , \tag{16}$$

where $v = 2t$ is the velocity and n is an integer. The Hamiltonian contains the usual free particle dispersion,

$$\mathcal{H} = -4t \sum_k \cos k \, c_k^\dagger c_k \ , \tag{17}$$

but the allowed k are given by eqn. (16). If the spectrum (near half-filling) is linearized around the Fermi momentum, $|k_F|$, then at small k states with nonzero a cost an additional energy of $(2\pi v/L)(a/N)^2$.

The a/N offset in k can be thought of as a minimally coupled vector potential such that the magnetic field is a δ-flux tube through the torus containing a/N flux quanta. In other words, one of the bonds along the chain (the anchor) had $\mathbf{Z}_N$ symmetry, whose effect is equivalent to a flux tube. Fig. 9 illustrates this equivalence.

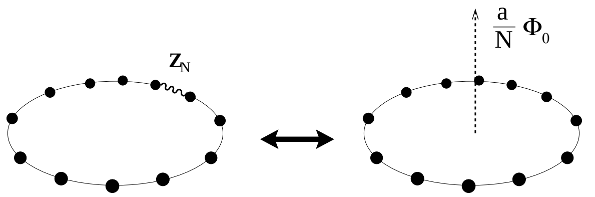

FIG. 9. The left ring shows the $\mathbf{Z}_N$ impurity on the anchor bond (wavy line). The right ring shows the equivalent alternative, where the impurity is replaced by a flux tube through the torus.

The offset in k due to the flux induces a total current in the fermion system.

At this point, one can see two topological effects on the torus. The first is the $\mathbf{Z}_N$ flux tube, or total current. As we have seen, its contribution to the energy near $|k_F|$ was $(2\pi v/L)(a/N)^2$. The second is the path winding along the length of the tube, or the total charge defined by eqn. (12). Its contribution to the energy near $|k_F|$ is similar, $(2\pi v/L)(bN/2)^2$. The total energy due to these topological sectors is

$$\Delta E_{a,b} = \frac{2\pi v}{L}\left(\frac{a^2}{N^2} + \frac{b^2 N^2}{4}\right) . \tag{18}$$

This expression is familiar from the Luttinger liquid model of one-dimensional spinless Fermions [19].

We can now obtain the continuum limit of our model. It is well known that free fermions in one dimension are equivalent to free bosons. The corresponding Lagrangian is

$$\mathcal{L} = \frac{1}{8\pi}[v^{-1}(\partial_t \varphi)^2 - v(\partial_x \varphi)^2] , \tag{19}$$

where φ is the bosonic field. $\mathcal{L}$ is a conformally invariant theory with central charge $c = 1$. We conjecture that the topological effects that we described above come from compactifying φ on a circle of radius R,

$$\phi \equiv \phi + 2\pi R . \tag{20}$$

By compactifying the boson, topological modes (or zero modes) appear. In field theory, they are conventionally obtained from electric and magnetic monopoles. The energy of the zero modes is

$$E^0_{a,b} = \frac{2\pi v}{L}\left(\frac{a^2}{R^2} + \frac{b^2 R^2}{4}\right) , \tag{21}$$

where a and b are integers labeling the fundamental cycles on the torus. Comparing $E^0_{a,b}$ (21) to $\Delta E_{a,b}$ (18), we find that $R = N$. The ordinary phonon (oscillator) modes exist on top of each topological sector and simply contribute the usual phonon energy, so that the complete dispersion is

$$E = E^0_{a,b} + \frac{2\pi}{L}|n| . \tag{22}$$

We have verified this energy spectrum by exact diagonalization for small systems in an earlier work [10].

The overall picture of a compactified boson with central charge $c = 1$ is consistent with the solid-on-solid models of Pasquier [17]. One can also ask what happens at higher order in t/V, which is the subject of the next subsection.

A. Finite t/V

The next corrections to $\mathcal{H}$ are of order t^2/V and involve virtual transitions to adatom configurations that are not in the degenerate subspace S. The generic form is

$$-\frac{t^2}{V}\mathcal{P}_S\left[\sum_{\langle ij\rangle\langle kl\rangle} b^\dagger_i b_j b^\dagger_k b_l\right]\mathcal{P}_S , \tag{23}$$

where $\mathcal{P}_S$ is a projection operator into S. Another way of writing the second order perturbation is the familiar form,

$$\langle\sigma'|\mathcal{H}|\sigma\rangle \to \langle\sigma'|\mathcal{H}|\sigma\rangle - \sum_\lambda \frac{\langle\sigma'|\mathcal{H}|\lambda\rangle\langle\lambda|\mathcal{H}|\sigma\rangle}{E_\lambda - E_\sigma} , \tag{24}$$

where $|\sigma\rangle, |\sigma'\rangle \in S$ while $|\lambda\rangle \notin S$ is the intermediate virtual state with energy E_λ. E_σ and $E_{\sigma'}$ are, of course, equal and constant, and all energy differences are due to the nearest neighbor repulsion $V n_i n_j$.

There are three types of virtual processes: (i) single particle hopping from σ to $\sigma \neq \sigma'$, (ii) two particle correlated hopping from σ to $\sigma \neq \sigma'$ and (iii) single particle diagonal hopping from σ back into σ. For concreteness, consider process (iii) in the $(5,0)$ state of fig. 8. Whenever there is a kink in σ, such as in the third layer from the top, the contribution to eqn. (24) from all virtual hops is $-(35/6)4t^2/V$. For example, the adatom on site 3 can hop into any one of its six neighbors with the energy denominators $1/2 + 1/2 + 1/2 + 1/2 + 1/2 + 1/3$ (in units of t^2/V). Similarly, the adatom on site 5 contributes $1 + 1 + 1$, for a total of $35/6$ (it is forbidden to hop one site over to the right because the resulting state is in S). On the other hand, if there is no kink, the contribution is $-8 \cdot 4t^2/V$. The criterion for a kink in layer i is $2[1/4 - (\tilde{n}_i - 1/2)(\tilde{n}_{i+1} - 1/2)] = 1$, where $\tilde{n}_i = c_i^\dagger c_i$ is the fermion number; otherwise this quantity vanishes. Similarly, the absence of a kink is synonymous with the nonvanishing of $2[1/4 + (\tilde{n}_i - 1/2)(\tilde{n}_{i+1} - 1/2)]$. Thus, the total diagonal contribution to $\mathcal{H}$ can be written

$$\begin{aligned}\mathcal{H} \to \mathcal{H} - \frac{8t^2}{V} \sum_\sigma \sum_i \left\{ \frac{35}{6} \left[\frac{1}{4} - \left(\tilde{n}_i - \frac{1}{2}\right)\left(\tilde{n}_{i+1} - \frac{1}{2}\right)\right] + 8 \left[\left(\tilde{n}_i - \frac{1}{2}\right)\left(\tilde{n}_{i+1} - \frac{1}{2}\right) + \frac{1}{4}\right] \right\} |\sigma\rangle\langle\sigma| \\ = \mathcal{H} - \frac{4t^2}{V} \sum_\sigma \left[\frac{13}{3} \sum_i \tilde{n}_i \tilde{n}_{i+1} - \frac{13}{3} \sum_i \tilde{n}_i + 8 \right] |\sigma\rangle\langle\sigma| \ . \qquad (25)\end{aligned}$$

For general N, the correction scales like N. The essential term in the last line of eqn. (25) is the first one. This four-fermion interaction renormalizes the radius R by corrections of order t/V.

Let us return to processes (i) and (ii). An example of (i) is the adatom in the third layer from the top, site 5, hopping to the second layer, site 1, and then back into the third layer, site 1. The intermediate state is not in S. This process serves only to renormalize t because its amplitude is the same for all kinks. An example of (ii) is the particle in the fourth layer, site 5, hopping to site 4, *followed by* the particle in the third layer, site 5, hopping to site 1 in the same layer. This correlated hopping occurs in a configuration containing the sequence particle-hole-hole or hole-particle-particle, which corresponds to a next-nearest neighbor interaction $c_{i+2}^\dagger c_{i+1}^\dagger c_{i+1} c_i + h.c.$. This type of term has a similar effect to the $\tilde{n}_i \tilde{n}_{i+1}$ term in eqn. (25), it reduces the value of R by corrections of order t/V. The four-fermion terms do not cancel unless there is a delicate cancellation.

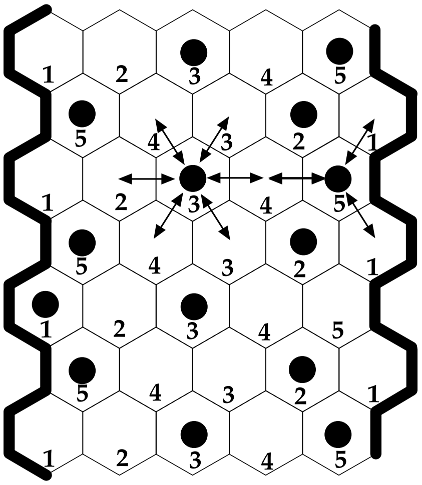

FIG. 10. An example of the virtual process (iii) in the configuration of Fig. 8.

One can also consider the extreme limit in which $t \gg V$. In this case, the XXZ Hamiltonian in eqn. (2) is simply the XY model on a cylinder. Note that our model has the particle-hole symmetry $t \leftrightarrow -t$ at least to order t^2/V. Let us denote the spin angle relative to the cylindrical surface by $\varphi(x, \theta)$, where x is the coordinate along the tube and θ is the coordinate around the perimeter. Uniqueness of the wavefunction requires that φ has the periodicity $\varphi(x, \theta + 2\pi) = \varphi(x, \theta) + 2\pi m$, where m is an integer. The low energy excitations are purely along the length of the tube; excitations around the perimeter will cost an energy on the order of $1/N$, which is large compared to $1/L$. Thus we can freeze the θ coordinate, and the energy density is proportional to $|\partial_x \varphi|^2$. Since the periodicity is still $\varphi \equiv \varphi + 2\pi m$, we end up with a free boson compactified on radius $R_{\text{XY}} = 1$. The question is how the adsorption regime $t \ll V$, which is also a compactified boson but on radius $R = N$, is reached.

B. The Lieb-Schultz-Mattis Argument

Another indication that our plateaus are nontrivial comes from trying to understand the spin tube as a spin ladder. Let us take this point of view to see if it yields the zero gap. A standard approach is to use a Lieb-Schultz-Mattis (LSM) argument, in which the spins are deformed slowly along the length [3]. Applying it to our tube, we find that a plateau is gapless if $\hat{S} - \hat{M}$ *is not* an integer, where $\hat{S}$ and $\hat{M}$ are the total spin and magnetization, respectively, per layer (a layer being the N sites around the perimeter). Using $\hat{S} = N/2$ and the magnetizations from Eqn. (8), we find that $\hat{S} - \hat{M}$ *is* an integer in the macroscopically degenerate plateaus, so that the LSM argument is insufficient in this case. Therefore, a conclusive argument must take the geometric frustration into account.

C. Special Case: $N = 2$

Before concluding with the effective theory, we should point out that the geometry of the $(2, 0)$ tube is special;

all sites in adjacent layers are interconnected. As a result, all of its plateaus have an extensive entropy, and we find that hopping opens a gap in both plateaus. Fig. 11 illustrates this exception. At either filling, the adatom in each layer is free to hop to either site—both configurations are iso-energetic because each site is contiguous to all sites in the neighboring layers. Hence both plateaus are macroscopically degenerate. In the presence of hopping, each adatom lives in a double well potential, which has a gap of order t. Therefore, neither plateau is gapless unlike higher N.

In fact, this tube can be written as a spin chain that has been studied at isotropic coupling [18], $-2t = V$. Two plateaus were found in this case, and it is tempting to speculate whether the two regimes are connected adiabatically.

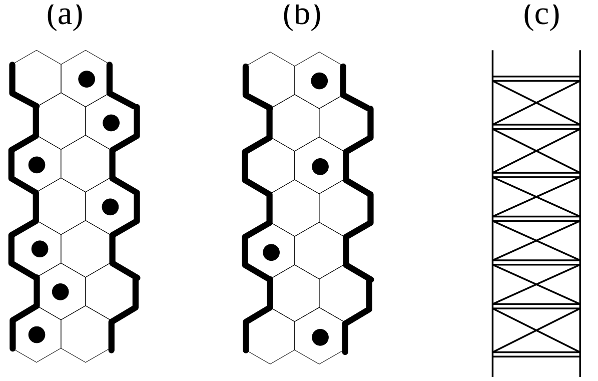

FIG. 11. The fillings for $N = 2$. $\nu_+ = 1/2$ (a) and $\nu_- = 1/4$ (b). Each adatom can live at either site in its layer because each site is connected to every site in the neighboring layers. (c) shows the triangular lattice in the plane; the horizontal double bond is due to the periodicity around a cylinder. (c) is exactly the geometry of the spin ladder studied by other authors (albeit with different coupling).

Another way to understand the gap is within the fermion model. Due to the high connectivity of the Bratteli diagram for $N = 2$, there is another allowed hop in addition to the $c_i^\dagger c_{i+1} + c_{i+1}^\dagger c_i$ term, which is $c_i^\dagger c_{i+1}^\dagger + c_{i+1} c_i$. This is a pairing interaction that leads to a superconducting gap.

IV. DISCUSSION AND CONCLUSION

In this paper we studied spin and Bose-Hubbard models in tube geometries. We found that an undelying frustrated triangular lattice, combined with extra geometric frustration from the closed topology of the tube, leads to interesting plateau structures for filling fractions ν (in the Bose-Hubbard models) or magnetizations $\langle M \rangle$ (for the spin models). In section II we studied the classical limit when the hopping t in the Bose-Hubbard model goes to zero; in the spin language, this correspond to the Ising limit. We obtained the different filling fractions allowed energetically by the wrapping condition, labelled by the vector (N, M). We showed that the corresponding solid phases are unique states, with the exception of the zig-zag tubes $(N, 0)$ with N not divisible by 3. In this particular case, which we studied in section II A, we showed that there is a macroscopic degeneracy of the classical ground state for a range of chemical potentials (or fields), *i.e.* a degenerate plateau. In contrast, when $N \equiv 0 \pmod 3$, there is only a single value of the chemical potential (or magnetic field, $H = 0$) for which the ground state degeneracy is non-trivial. We enumerated all the degenerate states at the plateau by mapping each state in the degenerate Hilbert space into a path in a Bratteli diagram wrapped on a cylinder. Using this enumeration, we then turned on the quantum hopping term t (or the XY spin couplings $J_\perp = 2t$) in section III. We found that the quantum terms lift up the degeneracy, leaving a gapless spectrum described by a $c = 1$ conformal field theory with compactification radius $R = N$. We presented an analytical argument that shows that the Bratteli path can be mapped into a state of a fermion model in a one dimensional chain, and the hopping terms in the tube lattice correspond to a hopping in the fermion chain. The compactification radius follows from a boundary $\mathbf{Z}_N$ degree of freedom and path winding, which must be included when the system is subject to periodic boundary conditions. We also discussed the cases when the anisotropy t/V (or $J_\perp/J_z$) is no longer small, and the special case $(N = 2, 0)$.

There are a number of interesting features that emerge from this problem of restricting spin and Bose-Hubbard Hamiltonians to tube geometries. For example, it is noteworthy that in the case of the $(N, 0)$ zig-zag tubes with N not divisble by 3, the low energy spectrum in the quantum case is gapless and described by a conformal field theory with a quantized compactification radius $R = N$; in the language of Luttinger liquids, this means that the Luttinger parameter is fixed by topology, similarly to the case of edge states in a fractional quantum Hall fluid [20], and in contrast to quantum wires (where the Luttinger parameter can vary continuously). In the spin tube problem, this quantization, in the projective limit $J_\perp \ll |J_z|$ (or $t \ll V$), follows simply from the fact that there is a direct connection between the physical lattice and the target space for the bosons. One of the interesting features of the spectrum for the gapless plateaus is that the specific heat is linear in temperature T, with the prefactor related to the velocity and a universal constant that depends on the central charge $c = 1$: $C = c\frac{\pi v k_B^2}{3} T = \frac{\pi v k_B^2}{3} T$. This dependence would be manifest in thermal measurements, and could be contrasted with exponentially activated behavior for the gapped solid phases.

Recently, there has been some interest in a connection that was pointed out by Kitaev [21] between the topological stability in some class of spin Hamiltonians in toroidal structures and quantum error correction for quantum computation. Bonesteel [22] investigated the possibility of using the two-fold topological degeneracy of spin-1/2 chiral spin liquid states on the torus to construct quantum error correcting codes. Since closed carbon nanotube structures (tori) have been observed experimentaly [23], it may be possible that spin tube geometries such as the ones discussed in this paper could realize physically some related Hamiltonians. We note, however, that for the class of Hamiltonians with nearest neighbor couplings that we studied here, there was only a trivial non-degenerate ground state, although there were topologically non-trivial excitations.

Finally, we would like to discuss a possible experimental set up for observing the filling fraction plateaus in the case of the monolayer adsorption problem of rare gases on the surface of carbon nanotubes. The filling fraction plateaus could be probed by measuring the resonance frequencies for a vibrating single wall carbon nanotube as a function of the vapor pressure of rare gas in a chamber. One way of measuring the resonant frequencies would be to have a single-wall tube hang alongside a multiwall tube, both with metallic grains at their tips. The multiwall tube is very stiff, and is basically rigid as compared to the single wall. By measuring the changes in the capacitance between the grains, one could probe the frequency of vibrations of the single-wall tube. This frequency is given by the square root of the ratio between the linear mass density and the stifness of the tube. Different filling fractions of adsorbed noble gases change the mass density of the tubes; however, their effect on the tube stiffness should be insignificant. The change in mass density of the nanotube due to adsorption of helium is basically $\delta\rho/\rho = \nu\ M_{\rm He}/2M_{\rm C} = \nu/12$. Hence, the ratio between the resonant frequencies $\omega_{1,2}$ for two plateaus at $\nu_{1,2}$ is

$$\frac{\omega_1}{\omega_2} = \sqrt{\frac{1+\frac{\nu_1}{12}}{1+\frac{\nu_2}{12}}} \approx 1 + \frac{\nu_1 - \nu_2}{24}\ . \qquad (26)$$

Resonant frequencies can be measured very precisely, so the filling fraction steps $\nu_1 - \nu_2$ should be experimentally measurable as a function of the vapor pressure of helium.

ACKNOWLEDGMENTS

The authors wish to thank C. Henley for interesting discussions, and N. Read for helpful comments and for pointing out Pasquier's work and the terminology of the Bratteli diagram. Support was provided by the NSF Grant DMR-98-18259 (D. G.), DMR-98-76208 and the Alfred P. Sloan Foundation (C. C.).

---

[1] K. Hida, J. Phys. Soc. Jpn. **63**, 2359 (1994).
[2] K. Okamoto, Solid State Commun. **98**, 245 (1996).
[3] M. Oshikawa, M. Yamanaka, and I. Affleck, Phys. Rev. Lett.**78**, 1984 (1997).
[4] D. C. Cabra, A. Honecker, P. Pujol, Phys. Rev. Lett. **79**, 5126 (1997).
[5] D. C. Cabra, A. Honecker, P. Pujol, Phys. Rev. B **58**, 6241 (1998).
[6] R. Citro, E. Orignac, N. Andrei, C. Itoi, S. Qin, J. Phys.: Condensed Matter **12**, 3041 (2000).
[7] E. Orignac, R. Citro and N. Andrei, cond-mat/9912200.
[8] Y. Narumi, M. Hagiwara, R. Sato, K. Kindo, H. Nakano, M. Takahashi, Physica B246-247, 509 (1998).
[9] W. Shiramura, K. Takatsu, B. Kurniawan, H. Tanaka, H. Uekusa, Y. Ohashi, K. Takizawa, H. Mitamura, T. Goto, J. Phys. Soc. Jpn. 67, 1548 (1998).
[10] D. Green and C. Chamon, Phys. Rev. Lett. **85**, 4128 (2000).
[11] M. Schick, J. S. Walker and M. Wortis, Phys. Rev. B **16**, 2205 (1977).
[12] M. Bretz, J. G. Dash, D. C. Hickernell, E. O. McLean, and O. E Vilches, Phys. Rev. B **8**, 1589 (1973).
[13] G. Murthy, D. Arovas, A. Auerbach, Phys. Rev. B **55**, 3104 (1997).
[14] *Interacting Electrons and Quantum Magnetism*, A. Auerbach, Springer-Verlag (1994).
[15] C. L. Henley and N. G. Zhang,cond-mat/0001411.
[16] P. Ginsparg in *Fields, Strings and Critical Phenomena*, E. Brezin and J. Zinn-Justin, eds., Elsevier (1988); J. L. Cardy, *ibid.*
[17] V. Pasquier, Nucl. Phys. **B285**, 162 (1987); V. Pasquier, J. Phys. **A20**, L1229 (1987).
[18] T. Sakai and N. Okazaki, cond-mat/0002113.
[19] F.D.M. Haldane, J. Phys. C **14**, 2585 (1981).
[20] X. G. Wen, Phys. Rev. B **41**, 12838 (1990).
[21] A.Y. Kitaev, e-print quant-ph/9707021
[22] N. E. Bonesteel, Phys. Rev. A **62**, 062310 (2000).
[23] R. Martel, H. R. Shea, and P. Avouris, Nature **398**, 299 (1999).